

1 **Trends of ambient fine particles and major chemical components in the Pearl**  
2 **River Delta region: observation at a regional background site in fall and winter**

3

4 Xiaoxin Fu<sup>1, 2</sup>, Xinming Wang<sup>1\*</sup>, Hai Guo<sup>2\*</sup>, Kalam Cheung<sup>2</sup>, Xiang Ding<sup>1</sup>, Xiuying Zhao<sup>1</sup>,  
5 Quanfu He<sup>1</sup>, Bo Gao<sup>1</sup>, Zhou Zhang<sup>1</sup>, Tengyu Liu<sup>1</sup>, Yanli Zhang<sup>1</sup>

6 <sup>1</sup>State Key Laboratory of Organic Geochemistry, Guangzhou Institute of Geochemistry, Chinese Academy of  
7 Sciences, Guangzhou 510640, China

8 <sup>2</sup>Air Quality Studies, Department Civil and Environmental Engineering, The Hong Kong Polytechnic University,  
9 Hong Kong

10

11 **\*Corresponding authors**

12 Hai Guo, ceguohai@polyu.edu.hk; Tel: +852 3400 3962; Fax: +852 23346389

13 Xinming Wang, wangxm@gig.ac.cn; Tel: +86 20 8529 0180; Fax: +86 20 8529 0706

14

15 **Abstract**

16 In the fall and winter of 2007 to 2011, 167 24-hr quartz filter-based fine particle (PM<sub>2.5</sub>) samples  
17 were collected at a regional background site in the central Pearl River Delta. The PM<sub>2.5</sub> showed an  
18 annual reduction trend with a rate of 8.58  $\mu\text{g m}^{-3}$  ( $p<0.01$ ). The OC component of the PM<sub>2.5</sub>  
19 reduced by 1.10  $\mu\text{g m}^{-3}$  per year ( $p<0.01$ ), while the reduction rates of sulfur dioxide (SO<sub>2</sub>) and  
20 sulfate (SO<sub>4</sub><sup>2-</sup>) were 10.2  $\mu\text{g m}^{-3} \text{ yr}^{-1}$  ( $p<0.01$ ) and 1.72  $\mu\text{g m}^{-3} \text{ yr}^{-1}$  ( $p<0.01$ ), respectively. In  
21 contrast, nitrogen oxides (NO<sub>x</sub>) and nitrate (NO<sub>3</sub><sup>-</sup>) presented growth trends with rates of 6.73  $\mu\text{g}$   
22  $\text{m}^{-3} \text{ yr}^{-1}$  ( $p<0.05$ ) and 0.79  $\mu\text{g m}^{-3} \text{ yr}^{-1}$  ( $p<0.05$ ), respectively. The PM<sub>2.5</sub> reduction was mainly  
23 related to the decrease of primary OC and SO<sub>4</sub><sup>2-</sup>, and the enhanced conversion efficiency of SO<sub>2</sub>  
24 to SO<sub>4</sub><sup>2-</sup> was related to an increase in the atmospheric oxidizing capacity and a decrease in aerosol  
25 acidity. The discrepancy between the annual trends of NO<sub>x</sub> and NO<sub>3</sub><sup>-</sup> was attributable to the small  
26 proportion of NO<sub>3</sub><sup>-</sup> in the total nitrogen budget.

27

28 **Key words:** PM<sub>2.5</sub>; Sulfate; Nitrate; Carbonaceous aerosols; Pearl River Delta

29

30 **Capsule abstract:** Understanding annual variations of PM<sub>2.5</sub> and its chemical composition is  
31 crucial in enabling policymakers to formulate and implement control strategies on particulate  
32 pollution.

## 33 **1. Introduction**

34 Many cities in China currently suffer severe air pollution problems, in particular haze caused by  
35 fine particles (PM<sub>2.5</sub>), resulting in visibility degradation and adverse health effects (Zhang et al.,  
36 2012a). Numerous heavy haze episodes have been observed in megacities such as Beijing,  
37 Shanghai, and Guangzhou in recent years (Wu et al., 2005; Sun et al., 2006; Fu et al., 2008;  
38 Chang et al., 2009). During these episodes, ambient PM<sub>2.5</sub> levels up to 466 µg/m<sup>3</sup> have been  
39 recorded, well over the World Health Organization (WHO) daily Air Quality Guidelines of 25  
40 µg/m<sup>3</sup>. High PM<sub>2.5</sub> levels are closely associated with long- and short-term health problems (Tie et  
41 al., 2009; van Donkelaar et al., 2010; Chen et al., 2012a; Shang et al., 2013). In an attempt to  
42 reduce particulate pollution, the Chinese government has recently implemented new national  
43 ambient air quality standards, which for the first time include PM<sub>2.5</sub>. Moreover, the government  
44 has emphasized the control of particulate pollution at a regional scale, with the main focus on the  
45 three economically relevant and densely populated city clusters; the North China Plain (NCP), the  
46 Yangtze River Delta (YRD) region, and the Pearl River Delta (PRD) region.

47 The PRD region in southern China makes up less than 1/200 of China's total land area but  
48 contributes about 10% of the nation's GDP, and is home to around 10% of its population. The  
49 ambient annual mean PM<sub>2.5</sub> level in this highly urbanized and industrialized region exceeded 100  
50 µg m<sup>-3</sup> in 2004 (Andreae et al., 2008). However, in recent years, the hazy days recorded a large  
51 drop from over 120 days in 2005 to less than 60 days in 2011 (<http://www.gzepb.gov.cn/>). Despite  
52 this reduction, average annual PM<sub>2.5</sub> levels in the PRD still exceed the daily and annual guidelines  
53 of the WHO. A systematic, long-term investigation into the variations in the main components of  
54 PM<sub>2.5</sub> and its mass concentrations will provide important information on sources and formation  
55 mechanisms, which will be useful in the formulating and implementing of particulate pollution  
56 control measures in the region, and also of value to other Chinese city clusters.

57 Over the last decade, studies have been conducted at different locations in the region on PM<sub>2.5</sub>  
58 mass concentrations and their major components, such as water soluble ions and carbonaceous  
59 aerosols (e.g. Lai et al., 2007; Hu et al., 2008; Tan et al., 2009a,b; Yang et al., 2011), and on the  
60 aerosols' light extinction and visibility impairment (Andreae et al., 2008; Jung et al., 2009; Tao et

61 [al., 2012](#)). However, the measurements were mainly carried out over short periods. Thus, the  
62 long-term variations in PM<sub>2.5</sub> mass concentrations and compositions were not determined. In this  
63 study, PM<sub>2.5</sub> filter samples were systematically collected from a background site in the region in  
64 fall and winter from 2007 and 2011 so that the annual trends of the mass concentrations and  
65 chemical components of PM<sub>2.5</sub> could be obtained.

## 66 **2. Experimental**

### 67 **2.1. Field sampling**

68 The PRD region has a typical Asian monsoon climate – hot and humid in the summer, with  
69 prevailing southwesterly monsoon winds from the sea, and relatively cool and dry in the fall and  
70 winter, when northeasterly monsoon winds from northern China dominate ([Ding and Chan, 2005](#)).

71 The region is often under the influence of high pressure ridges in the fall and winter, causing long  
72 periods of sunny days, with a low boundary layer and a high frequency of inversion. This stable  
73 meteorological condition facilitates the accumulation of pollutants and a resulting deterioration of  
74 air quality. As a result, high levels of air pollutants usually occur in fall and winter ([Fan et al.,  
75 2008; Liu et al., 2008](#)). Field measurements were thus collected in those two seasons each year.

76 The sampling site, Wanqingsha (WQS: 22.42° N, 113.32° E), was located in a small town south  
77 of Guangzhou, in the center of the PRD ([Figure 1](#)). The town was surrounded by farmland, has  
78 little traffic, and very few textile and clothing workshops. The local anthropogenic emissions  
79 were thus not significant, with most air pollutants originating from the surrounding cities. The site  
80 was 50 km southeast of Guangzhou center, 40 km southwest of Dongguan, 50 km northwest of  
81 Shenzhen, and 25 km northeast of Zhongshan, making it a good regional station to characterize  
82 the air pollution of the inner PRD ([Guo et al., 2009](#)). The PM<sub>2.5</sub> high-volume samplers ([Tisch  
83 Environmental Inc., USA](#)) were placed on the rooftop of a building, about 30 m above the ground.  
84 Gas-phase pollutants, including SO<sub>2</sub> and NO<sub>x</sub>, were also monitored.

85 The 24-hr PM<sub>2.5</sub> samples were collected by drawing air through an 8×10 inch quartz filter ([QMA,  
86 Whatman, UK](#)) at a rate of 1.1 m<sup>3</sup> min<sup>-1</sup>. The filters were pre-baked at 450°C for four hours,  
87 wrapped in aluminum foil, zipped in Teflon bags, and stored at –20°C before sampling. They  
88 were again stored in this way after sample collection. In 2007, 2008, 2009, 2010, and 2011, 32, 29,

89 25, 53, and 28 samples were collected, respectively. The meteorological parameters were  
90 measured by a mini weather station ([Vantage Pro2™, Davis Instruments Corp., USA](#)) with wind  
91 speed/direction, relative humidity (RH), and temperature recorded every minute.

## 92 **2.2. Chemical analysis**

93 The PM<sub>2.5</sub> filters were weighted before and after field sampling, after 24-hr equilibrium, at a  
94 temperature of 20-23°C and with a RH between 35-45%. The organic carbon (OC) and elemental  
95 carbon (EC) in the PM<sub>2.5</sub> were determined by the thermo-optical transmittance (TOT) method  
96 ([NIOSH, 1999](#)) using an OC/EC analyzer ([Sunset Laboratory Inc., USA](#)), with a punch (1.5×1.0  
97 cm) of the sampled filters. For the water-soluble inorganic ions, a punch (5.06 cm<sup>2</sup>) of the filters  
98 was extracted twice with 10 ml ultrapure Milli-Q water (18.2 MΩ·cm/25°C) each for 15 min  
99 using an ultrasonic ice-water bath. The total water extracts (20 ml) were filtered through a 0.22  
100 μm pore size filter and then stored in a pre-cleaned HDPE bottle. The cations (i.e. Na<sup>+</sup>, NH<sub>4</sub><sup>+</sup>, K<sup>+</sup>,  
101 Mg<sup>2+</sup>, and Ca<sup>2+</sup>) and anions (i.e. Cl<sup>-</sup>, NO<sub>3</sub><sup>-</sup>, and SO<sub>4</sub><sup>2-</sup>) were analyzed with an ion-chromatography  
102 system ([Metrohm, 883 Basic IC plus](#)). Cations were measured using a Metrohm Metrosep  
103 C4-100 column with 2 mmol L<sup>-1</sup> sulfuric acid as the eluent. Anions were measured using a  
104 Metrohm Metrosep A sup5-150 column equipped with a suppressor. The anion eluent was a  
105 solution of 3.2 mmol L<sup>-1</sup> Na<sub>2</sub>CO<sub>3</sub> and 1.0 mmol L<sup>-1</sup> NaHCO<sub>3</sub>.

## 106 **2.3. Quality assurance / quality control (QA/QC)**

107 Field and laboratory blank samples were analyzed in the same way as field samples. All the OC/EC  
108 and cation/anion data were corrected using the field blanks. The method detection limits (MDLs)  
109 were 0.01-0.05 μg m<sup>-3</sup> for the OC, EC, cations, and anions. Ions balance was used as a quality  
110 control check in the cation/anion analysis. Nano-equivalents of cations and anions were calculated  
111 using their mass concentrations and molecular weights:

$$112 \text{ Cation nano-equivalents (CE)} = (\text{Na}^+/23 + \text{NH}_4^+/18 + \text{K}^+/39 + \text{Mg}^{2+}/24 \times 2 + \text{Ca}^{2+}/40 \times 2) \times 1000 \quad (1)$$

$$113 \text{ Anion nano-equivalents (AE)} = (\text{Cl}^-/35.5 + \text{NO}_3^-/62 + \text{SO}_4^{2-}/96 \times 2) \times 1000 \quad (2)$$

114 A significant linear correlation ( $R^2=0.984$ ) was observed between CE and AE ([Figure 2](#)) with a  
115 slope of 1.14 for all PM<sub>2.5</sub> samples. This slope was close to identity and indicated that all the  
116 significant ions were resolved. The AE/CE slope was slightly higher than 1.0, suggesting that the

117 aerosols in WQS tended to be acidic (Seinfeld and Pandis, 2006).

### 118 3. Results and discussion

#### 119 3.1 PM<sub>2.5</sub> mass concentrations

120 The PM<sub>2.5</sub> concentration in the fall and winter of 2007-2011 ranged from 22.3 (December 2010) to  
121 191  $\mu\text{g m}^{-3}$  (November 2010) with an average of  $95.2 \pm 4.49 \mu\text{g m}^{-3}$  (average  $\pm$  95% Confidence  
122 Interval). Table 1 shows that the PM<sub>2.5</sub> level significantly decreased from  $112.5 \pm 8.2 \mu\text{g m}^{-3}$  in  
123 2007 to  $78.6 \pm 7.6 \mu\text{g m}^{-3}$  in 2011 ( $p < 0.01$ ), with a slope of  $-8.58 \mu\text{g m}^{-3} \text{ yr}^{-1}$ , or an average  
124 reduction rate of  $8.6\% \text{ yr}^{-1}$  (Figure 3). This reflected the efficient reduction of PM<sub>2.5</sub> pollution in  
125 these years. The Guangdong government implemented various control measures, such as the  
126 increased use of nuclear and hydroelectric power; the phasing out of small coal-fired power  
127 generation units; prohibiting the building of new cement plants, ceramics factories, and  
128 glassworks; the establishment of stricter emission standards for industrial boilers, and  
129 improvements in the quality of vehicle fuel (<http://www.gzepb.gov.cn/>). The decreasing trend of  
130 PM<sub>2.5</sub> is consistent with the yearly PM<sub>10</sub> variations measured in the region. The PM<sub>10</sub> was  
131 measured at the same site by the Guangdong Environmental Monitoring center during fall and  
132 winter from 2007 to 2011, and fell from  $147 \mu\text{g m}^{-3}$  in 2007 to  $91 \mu\text{g m}^{-3}$  in 2011, with an average  
133 reduction rate of  $11.8 \mu\text{g m}^{-3} \text{ yr}^{-1}$  or  $-10.3\% \text{ yr}^{-1}$  ([http://www.epd.gov.hk/epd/english/resources](http://www.epd.gov.hk/epd/english/resources_pub/publications/m_report.html)  
134 [\\_pub/publications/m\\_report.html](http://www.epd.gov.hk/epd/english/resources_pub/publications/m_report.html)). Comparable or higher PM<sub>2.5</sub> concentrations were observed at  
135 urban sites in the same region. For instance, Tan et al. (2009a) found that PM<sub>2.5</sub> concentration was  
136  $171.7 \mu\text{g m}^{-3}$  in January 2008, Yang et al. (2011) recorded  $81.7 \pm 25.6 \mu\text{g m}^{-3}$  (average  $\pm$  standard  
137 deviation) in December 2008 to February 2009, and Tao et al. (2012) recorded  $103.3 \pm 50.1 \mu\text{g}$   
138  $\text{m}^{-3}$  in January 2010. The PM<sub>2.5</sub> values in the PRD region were, however, much higher than those  
139 observed in central California ( $13.5 \mu\text{g m}^{-3}$ ) (Rinehart et al., 2006), in Spain ( $9.0 \mu\text{g m}^{-3}$ ), and in  
140 Germany ( $10 \mu\text{g m}^{-3}$ ) (Cusack et al., 2012). In contrast, emission estimate studies conducted in the  
141 PRD region found the opposite change in PM<sub>2.5</sub> emissions. Zheng et al. (2009, 2012a) reported  
142 that the PM<sub>2.5</sub> emission was 205 Gg in 2006 and 303 Gg in 2009, for example.

143 Among all of the PM<sub>2.5</sub> samples, only one was below the WHO 24-hr guideline level of  $25 \mu\text{g m}^{-3}$   
144 and three were below the US EPA 24-hr standard of  $35 \mu\text{g m}^{-3}$ , and 75% of the samples were

145 above the Chinese daily standard of  $75 \mu\text{g m}^{-3}$  (Figure 4) (GB 3095-2012,  
146 [http://kjs.mep.gov.cn/hjbhbz/bzwb/dqhjbh/dqhjzlbz/201203/t20120302\\_224165.htm](http://kjs.mep.gov.cn/hjbhbz/bzwb/dqhjbh/dqhjzlbz/201203/t20120302_224165.htm)). The  
147 maximum concentration of  $191 \mu\text{g m}^{-3}$  was on November 6, 2010, with the rehearsal of the  
148 large-scale firework display for the opening ceremony of the 16<sup>th</sup> Asia games. Elevated  $\text{PM}_{2.5}$   
149 levels were also recorded during the opening ceremony of the 10<sup>th</sup> Asian Games for the Disabled  
150 ( $163.9 \mu\text{g m}^{-3}$  on December 12, 2010), and on the day after the closing ceremony ( $174.9 \mu\text{g m}^{-3}$   
151 on December 20, 2010), reflecting the significant effect of burning fireworks. Indeed, Wang et al.  
152 (2007) stated that during the Chinese Lantern Festival in Beijing, when many fireworks were set  
153 off,  $\text{SO}_4^{2-}$  and  $\text{NO}_3^-$  levels were over five times higher than normal. The lowest  $\text{PM}_{2.5}$   
154 concentration ( $22.3 \mu\text{g m}^{-3}$ ) occurred on December 15, 2010, when a strong intrusion of cold air  
155 masses from the north caused a sudden temperature drop, and air pollutants swept into the region.  
156 **In recent years, fine particle pollution has significantly reduced in the PRD region, but further**  
157 **efforts are necessary to reduce  $\text{PM}_{2.5}$  emissions.**

### 158 **3.2 Chemical compositions of $\text{PM}_{2.5}$**

159 The concentrations of carbonaceous aerosols and water soluble ions in  $\text{PM}_{2.5}$ , the ratios of OC/EC,  
160  $\text{NH}_4^+/\text{SO}_4^{2-}$ , and  $\text{NO}_3^-/\text{SO}_4^{2-}$ , and the meteorological conditions over the five year period are listed  
161 in Table 1. Figure 5 shows the chemical components of  $\text{PM}_{2.5}$  in the same period. The aerosol  
162 organic matter (OM) equals  $2 \times \text{OC}$  (Wang et al., 2012a). OM was the most abundant component  
163 over this period. The average OC concentration was highest in 2008 ( $22.7 \pm 2.93 \mu\text{g m}^{-3}$ ; average  
164  $\pm 95\%$  CI) and lowest in 2011 ( $15.2 \pm 2.06 \mu\text{g m}^{-3}$ ). For EC, the average concentration was  
165 highest in 2009 ( $5.5 \pm 0.90 \mu\text{g m}^{-3}$ ) and lowest in 2011 ( $3.1 \pm 0.38 \mu\text{g m}^{-3}$ ). These  $\text{PM}_{2.5}$   
166 component levels approximated those recorded in the winter in urban Guangzhou, i.e.  $26.8 \mu\text{g m}^{-3}$   
167 for OC and  $6.2 \mu\text{g m}^{-3}$  for EC in January 2008 (Tan et al., 2009a),  $17.5 \pm 7.6 \mu\text{g m}^{-3}$  (average  $\pm$   
168 SD) for OC and  $4.1 \pm 2.0 \mu\text{g m}^{-3}$  for EC in the winter of 2008-2009 (Yang et al., 2011), and  $11.8 \pm$   
169  $7.3 \mu\text{g m}^{-3}$  for OC and  $7.8 \pm 4.3 \mu\text{g m}^{-3}$  for EC in January 2010 (Tao et al., 2012). However, the  
170 OC and EC concentrations measured in this study were much higher than those observed in urban  
171 Paris in 2009-2010 (OC:  $3.0 \pm 1.7 \mu\text{g m}^{-3}$  and EC:  $1.4 \pm 0.7 \mu\text{g m}^{-3}$  (average  $\pm$  SD)) (Bressi et al.,  
172 2013), and in both residential and commercial areas of Incheon, Korea, (OC:  $10.9 \pm 0.8 \mu\text{g m}^{-3}$

173 and EC:  $1.8 \pm 0.1 \mu\text{g m}^{-3}$ ) in the winter of 2009-2010 (Choi et al., 2012).  
174 Concentrations of  $\text{SO}_4^{2-}$  ranged from  $22.7 \pm 2.3 \mu\text{g m}^{-3}$  (average  $\pm$  95% CI) in 2007 to  $14.2 \pm 1.8$   
175  $\mu\text{g m}^{-3}$  in 2011, while the average  $\text{NO}_3^-$  concentrations increased from  $6.7 \pm 1.1 \mu\text{g m}^{-3}$  in 2007 to  
176 a peak of  $11.5 \pm 1.9 \mu\text{g m}^{-3}$  in 2009, and then decreased to  $9.6 \pm 1.5 \mu\text{g m}^{-3}$  in 2011. The  $\text{NH}_4^+$   
177 concentrations did not show a significant change over the five year period. As with  $\text{PM}_{2.5}$ , the  
178 fireworks of November 6, 2010 resulted in  $\text{SO}_4^{2-}$ ,  $\text{NO}_3^-$ , and  $\text{NH}_4^+$  concentrations reaching their  
179 maxima, with levels of 40.2, 41.4, and  $24.4 \mu\text{g m}^{-3}$ , respectively. High  $\text{SO}_4^{2-}$ ,  $\text{NO}_3^-$ , and  $\text{NH}_4^+$   
180 values have been recorded on hazy days in various Chinese megacities. For example, at an urban  
181 site in Beijing, levels reached 24.8, 49.3, and  $26.2 \mu\text{g m}^{-3}$ , respectively in October 2010, and  
182 28.11, 42.46 and  $18.32 \mu\text{g m}^{-3}$  in October 2011 (Sun et al., 2013). In Shanghai, levels of 28.7, 32.9,  
183 and  $19.3 \mu\text{g m}^{-3}$  were recorded in May-June 2009 (Du et al., 2011). By contrast, recorded  
184 concentrations of  $\text{SO}_4^{2-}$ ,  $\text{NO}_3^-$ , and  $\text{NH}_4^+$  were much lower in US and European cities. The  
185 average concentrations in the southeastern US were over five times lower than those found in  
186 WQS (Chen et al., 2012b), and in Spain in 2002-2010 levels as low as 2.4, 1.0 and  $1.0 \mu\text{g m}^{-3}$   
187 were recorded (Cusack et al., 2012).

188 The  $\text{NO}_3^-/\text{SO}_4^{2-}$  ratio could indicate the contribution of mobile and stationary sources to sulfur  
189 and nitrogen in the atmosphere (Arimoto et al., 1996). The mass ratio of  $\text{NO}_3^-/\text{SO}_4^{2-}$  rose from  
190  $0.31 \pm 0.06$  (average  $\pm$  95% CI) in 2007 to  $0.58 \pm 0.10$  in 2008, and reached  $0.69 \pm 0.11$  during  
191 2009-2011. A previous study reported a  $\text{NO}_3^-/\text{SO}_4^{2-}$  mass ratio of 2-5 in Los Angeles, and in  
192 Rubidoux in southern California, where very little coal burning occurred (Kim et al., 2000). The  
193  $\text{NO}_3^-/\text{SO}_4^{2-}$  mass ratios in this study increased from 2007 to 2011, but they were all less than 1.0,  
194 and therefore much lower than those of Los Angeles and Rubidoux, indicating the effect of  
195 stationary sources (coal combustion) in the PRD region (Yao et al., 2002; Wang et al., 2005; Cao  
196 et al., 2009). The mole ratio of  $[\text{NH}_4^+]$  to  $(2 \times [\text{SO}_4^{2-}] + [\text{NO}_3^-])$  increased from  $0.64 \pm 0.04$  in 2007  
197 to  $0.80 \pm 0.02$  in 2011, suggesting that aerosol acidity decreased over the five year period.

### 198 3.3. Annual trends of major components in $\text{PM}_{2.5}$

#### 199 3.3.1 Sulfate ( $\text{SO}_4^{2-}$ )

200 Figure 6 (a) shows that on average,  $\text{SO}_4^{2-}$  decreased at a rate of  $1.72 \mu\text{g m}^{-3} \text{ yr}^{-1}$  or  $11.0\% \text{ yr}^{-1}$  ( $p <$



201 0.01), whereas for SO<sub>2</sub> the reduction was 10.2 μg m<sup>-3</sup> or 18.8% a year ( $p < 0.01$ ). SO<sub>2</sub>  
202 concentrations thus decreased much more rapidly than SO<sub>4</sub><sup>2-</sup>. Our data showed that each 1%  
203 reduction in SO<sub>2</sub> concentration resulted in a 0.59% (i.e. 11.0% divided by 18.8%) decrease in  
204 SO<sub>4</sub><sup>2-</sup> concentration in the PRD region (i.e. a 1 μg m<sup>-3</sup> change in SO<sub>2</sub> caused a 0.17 μg m<sup>-3</sup> change  
205 in SO<sub>4</sub><sup>2-</sup>). The decreasing trends of SO<sub>2</sub> and SO<sub>4</sub><sup>2-</sup> found are in line with previous studies. Based  
206 on satellite retrieval data, Zhang et al. (2012b) found the yearly average tropospheric SO<sub>2</sub> vertical  
207 columns in the PRD region decreased from 0.223 ± 0.135 DU (average ± SD) in 2006 to 0.144 ±  
208 0.064 DU in 2009 with a reduction rate of 11.8% yr<sup>-1</sup>, while Lu et al. (2013) reported that  
209 normalized SO<sub>2</sub> emissions significantly decreased between 2007 and 2009, at a rate of 15.4% yr<sup>-1</sup>.  
210 Previous studies have also reported the relationship between decreased concentrations of SO<sub>2</sub> and  
211 SO<sub>4</sub><sup>2-</sup>. Holland et al. (1999) found that SO<sub>2</sub> concentrations decreased by 35% and SO<sub>4</sub><sup>2-</sup>  
212 concentrations by 26% in the eastern US from 1989 to 1995. In Finland, France, and Germany,  
213 observed SO<sub>4</sub><sup>2-</sup> concentrations decreased by 85-70% as SO<sub>2</sub> concentrations decreased by 85-90%,  
214 between 1980 and 2000 (Lovblad et al., 2004). Manktelow et al. (2007) used a global model to  
215 investigate changes in the regional sulfur budget from 1985 to 2000. Their findings were similar  
216 to ours, and for every 1% decrease in SO<sub>2</sub> surface concentration, SO<sub>4</sub><sup>2-</sup> surface concentration  
217 decreased by 0.55% across Western Europe, and by 0.58% across the US. The different response  
218 was due to the fact that conversion efficiency of SO<sub>2</sub> to SO<sub>4</sub><sup>2-</sup> in clouds increased when SO<sub>2</sub>  
219 emissions decreased. The much higher reduction rate of SO<sub>2</sub> found in the PRD region implied that  
220 the control measures of the time were effective. The main source of SO<sub>2</sub> in China was coal-fired  
221 power plants (Zhao et al., 2008; Lu et al., 2010), and after the installation and operation of flue  
222 gas desulfurization (FGD) systems in thermal power units and the closure of small and  
223 less-efficient power plants, the total industrial SO<sub>2</sub> emission in Guangdong dropped from 1,203  
224 Gg in 2007 to 848 Gg in 2011, with a decreasing rate of 7.4% yr<sup>-1</sup> (GPBS, 2008-2012). The faster  
225 rate of decrease was also related to the atmospheric chemistry of sulfur. SO<sub>4</sub><sup>2-</sup> is produced from  
226 the dry oxidation between SO<sub>2</sub> and the OH radical, and/or from the oxidation of SO<sub>2</sub> by H<sub>2</sub>O<sub>2</sub> and  
227 O<sub>3</sub> through in-cloud processes. H<sub>2</sub>O<sub>2</sub> is the most dominant oxidant of SO<sub>2</sub> in atmospheric aqueous  
228 phases, particularly when the pH is lower than 5 (Calvert et al., 1985). In the PRD region, H<sub>2</sub>O<sub>2</sub>

229 was significant in the formation of sulfate in the aerosol phase (Hua et al., 2008). The intensity of  
230 solar radiation is a significant factor, as it controls the atmospheric oxidizing capacity (Merkel et  
231 al., 2011; Wang et al., 2012b). Furthermore, H<sub>2</sub>O<sub>2</sub> positively correlates with solar radiation (Acker  
232 et al., 2008; Marinoni et al., 2011). In recent years, PM<sub>2.5</sub> concentrations have significantly  
233 decreased in the PRD, resulting in enhanced solar radiation and actinic flux in the troposphere.  
234 Hence, the conversion efficiency of SO<sub>2</sub> to SO<sub>4</sub><sup>2-</sup> in clouds over the region is even more rapid.  
235 The equilibriums of SO<sub>2</sub> dissolving, which lead to the formation of bisulfite and sulfite ions in the  
236 presence of particle phase, are sensitive to the pH value. The aerosol acidity (mole ratio of [NH<sub>4</sub><sup>+</sup>]  
237 to (2 × [SO<sub>4</sub><sup>2-</sup>] + [NO<sub>3</sub><sup>-</sup>])) in the five year period decreased by 25% in 2011, compared to the ratio  
238 in 2007, where the solubility of SO<sub>2</sub> was enhanced and certain oxidation processes were  
239 accelerated (Jones and Harrison, 2011). In conclusion, the rapid reduction of SO<sub>2</sub> was caused by  
240 the decrease in the source emissions and by the enhanced conversion efficiency of SO<sub>2</sub> to SO<sub>4</sub><sup>2-</sup>  
241 through in-cloud processes, due to the increased oxidizing capacity and the drop in aerosol acidity  
242 in this period. Consequently, the combined effect of these factors led to the slow decreasing trend  
243 of SO<sub>4</sub><sup>2-</sup> in the region.

### 244 3.3.2 Nitrate (NO<sub>3</sub><sup>-</sup>)

245 The observed NO<sub>3</sub><sup>-</sup> levels increased at a rate of 0.79 μg m<sup>-3</sup> yr<sup>-1</sup> or 9.5% yr<sup>-1</sup> ( $p < 0.05$ ), and NO<sub>x</sub>  
246 on average increased by 6.73 μg m<sup>-3</sup> or 9.8% every year ( $p < 0.05$ ) (Figure 6(b)). The NO<sub>x</sub>  
247 concentrations increased more rapidly than those of the NO<sub>3</sub><sup>-</sup>. Specifically, every 1% increase in  
248 NO<sub>x</sub> concentration resulted in a 0.97% increase in NO<sub>3</sub><sup>-</sup> concentration in the PRD region.

249 It is well known that power plants, factories, and vehicles were major contributors of NO<sub>x</sub>  
250 emissions in China (Streets et al., 2003; Ohara et al., 2007; Gu et al., 2012). Electricity production  
251 in the PRD region grew at a rate of 12.7 % yr<sup>-1</sup> during 2007-2011 (GPBS, 2008-2012), which led  
252 to an increase in NO<sub>x</sub> emission from 392 Gg in 2005 to 586 Gg in 2010; an increase rate of 9.9 %  
253 yr<sup>-1</sup> (Zhao et al., 2008). The number of vehicles in Guangdong increased from 5.07 million in  
254 2007 to 9.12 million in 2011, a striking growth rate of 20% yr<sup>-1</sup> (GPBS, 2008-2012), which also  
255 contributed to the NO<sub>x</sub> emission increase. Power plants in Guangdong, however, were obliged to  
256 use low-NO<sub>x</sub> burner technologies and denitrification facilities after the implementation of

257 emission standards for coal-fired power plants in 2009. Thus, the effort to control NO<sub>x</sub> emission  
258 from coal-fired power plants in the PRD region over the study period was counteracted by the  
259 rapid growth in power generation and in motor vehicle numbers.

260 Combustion sources emit NO<sub>x</sub>, and involve a series of chemical reactions producing organic and  
261 inorganic nitrate compounds, including NO<sub>3</sub><sup>-</sup>. The nitrogen chemistry in the atmosphere results in  
262 both NO<sub>3</sub><sup>-</sup> and NO<sub>x</sub> generating organic nitrates (i.e. RONO<sub>2</sub>), peroxyacetyl nitrate (PAN), HNO<sub>3</sub>  
263 (gas), nitrous acid (HONO), and reactive intermediates, which are difficult to detect but are  
264 extremely important for the nitrogen budget (Atkinson, 2000). The total level of C<sub>1</sub>–C<sub>5</sub> alkyl  
265 nitrates (RONO<sub>2</sub>) reached about 0.35 μg m<sup>-3</sup> at a coastal site of Hong Kong in November 2002  
266 (Simpson et al., 2006), while the highest concentration of PAN in the PRD was 19.3 μg m<sup>-3</sup> in the  
267 summer of 2006, equal to the level of NO<sub>3</sub><sup>-</sup> found in this study (Wang et al., 2010). The average  
268 concentrations of HNO<sub>3</sub> and HONO in the PRD region in October–November 2004 were 6.3 and  
269 2.9 μg m<sup>-3</sup>, respectively (Hu et al., 2008). In general, NO<sub>3</sub><sup>-</sup> only accounted for a small proportion  
270 of NO<sub>x</sub> products, which is why this study found that the NO<sub>x</sub> concentrations increased more  
271 rapidly than NO<sub>3</sub><sup>-</sup>.

272 **In summary, the increase in NO<sub>x</sub> emissions from coal-fired power plants and vehicles in recent**  
273 **years suggests that future NO<sub>x</sub> reduction in the region will be a major challenge. As the precursor**  
274 **of ozone in the troposphere, NO<sub>x</sub> increase leads to an alteration in atmospheric oxidizing capacity,**  
275 **and subsequently affects the formation of secondary components of PM<sub>2.5</sub>.**

### 276 **3.4 Elemental carbon (EC) and Organic carbon (OC)**

277 **Figure 7 (a)** shows there was no clear decreasing trend in EC over this time ( $p = 0.06$ ), perhaps  
278 due to the combined effect of residential, industrial, and vehicular emissions. The main EC  
279 sources in the PRD were residential and industrial emissions, transportation, and biomass burning  
280 (Cao et al., 2006; Lei et al., 2011; Qin and Xie, 2012). During 2007–2011, the total annual  
281 residential coal usage decreased, whereas the consumption of liquefied petroleum gas and  
282 household electricity increased. Moreover, industrial EC emission reduced from 27.3 Gg in 2007  
283 to 26.4 Gg in 2011, with an annual reduction rate of 0.8% (GPBS, 2008–2012). In contrast, the  
284 rapid increase in vehicle numbers in the region increased EC emissions, offsetting the industrial

285 and residential decrease.

286 A higher decreasing rate of OC (i.e.  $1.10 \mu\text{g m}^{-3}\text{yr}^{-1}$  or  $5.9\% \text{ yr}^{-1}$ ) ( $p < 0.01$ ) was found in this  
287 period (Figure 7(b)). OC is composed of primary OC (POC) and secondary OC (SOC). The SOC  
288 was estimated using the EC-tracer method (Turpin and Huntzicker, 1995), and the POC was the  
289 difference between OC and SOC. Figures 8(a) and (b) show that POC levels decreased at a rate of  
290  $0.74 \mu\text{g m}^{-3} \text{ yr}^{-1}$  ( $p < 0.01$ ), whereas SOC did not show a significant decreasing trend ( $p = 0.17$ ).  
291 The average proportion of POC and SOC in OC was 60.9% and 39.2%, respectively. Hence, POC  
292 was the major component of OC, and the OC reduction was mainly attributed to the decrease in  
293 POC emissions. The unchanged SOC levels during the study period might indicate a potential  
294 impediment to further  $\text{PM}_{2.5}$  reduction in the region.

#### 295 4. Conclusions

296  $\text{PM}_{2.5}$  mass concentrations and its chemical components were measured at a site in the central  
297 PRD region in fall and winter from 2007 to 2011. There was a significant annual reduction rate of  
298  $\text{PM}_{2.5}$  of  $8.58 \mu\text{g m}^{-3} \text{ yr}^{-1}$ . In  $\text{PM}_{2.5}$ , OC and  $\text{SO}_4^{2-}$  decreased  $1.10 \mu\text{g m}^{-3}$  and  $1.72 \mu\text{g m}^{-3}$  per year,  
299 respectively. By contrast,  $\text{NO}_3^-$  displayed an increasing rate of  $0.79 \mu\text{g m}^{-3} \text{ yr}^{-1}$ . In general,  $\text{PM}_{2.5}$   
300 reduction in the PRD region was mainly due to the reduction of OM and  $\text{SO}_4^{2-}$ .  $\text{SO}_2$  had a  
301 decreasing rate of  $10.2 \mu\text{g m}^{-3} \text{ yr}^{-1}$ , while  $\text{NO}_x$  presented a growth rate of  $6.73 \mu\text{g m}^{-3} \text{ yr}^{-1}$ . The  
302 precursors  $\text{SO}_2$  and  $\text{NO}_x$  concentrations obviously decreased and increased more rapidly than  
303  $\text{SO}_4^{2-}$  and  $\text{NO}_3^-$ . The faster reduction of  $\text{SO}_2$  than  $\text{SO}_4^{2-}$  was associated with the combined  
304 influence of decreased source emissions, increased oxidizing capacity with cloud processes, and  
305 reduced aerosol acidity. In contrast, the more rapid increase in  $\text{NO}_x$  concentration than that of  
306  $\text{NO}_3^-$  was likely due to increased power generation and vehicle numbers, which offset efforts to  
307 control coal-fired power plants, and  $\text{NO}_x$  was converted into  $\text{NO}_3^-$  and other nitrogen compounds.  
308 Although air pollution caused by  $\text{PM}_{2.5}$  has been reduced in the PRD region in recent years, the  
309 reduction of fine particle emissions, particularly  $\text{NO}_3^-$  and SOC, will be extremely challenging in  
310 the future.

#### 311 Acknowledgments

312 This study was supported by the National Natural Science Foundation of China (Project No.

313 41025012), the Strategic Priority Research Program of the Chinese Academy of Sciences (Grant  
314 No. XDB05010200), the Research Grants Council of the Hong Kong government  
315 (PolyU5154/13E), and the joint supervision scheme of the Hong Kong Polytechnic University  
316 (G-UB67).

## 317 **References**

- 318 Acker, K., Kezele, N., et al., 2008. Atmospheric H<sub>2</sub>O<sub>2</sub> measurement and modeling campaign  
319 during summer 2004 in Zagreb, Croatia. *Atmospheric Environment* 42, 2530-2542.
- 320 Andreae, M.O., Schmid, O., Yang, H., Chand, D., Yu, J.Z., Zeng, L.M., Zhang, Y.H., 2008.  
321 Optical properties and chemical composition of the atmospheric aerosol in urban Guangzhou,  
322 China. *Atmospheric Environment* 42, 6335-6350.
- 323 Arimoto, R. et al., 1996. Relationships among aerosol constituents from Asia and the North  
324 Pacific during PEM-West A. *Journal of Geophysical Research-Atmospheres* 101, 2011-2023.
- 325 Atkinson, R., 2000. Atmospheric chemistry of VOCs and NO<sub>x</sub>. *Atmospheric Environment* 34,  
326 2063-2101.
- 327 Bressi, M. et al., 2013. A one-year comprehensive chemical characterisation of fine aerosol (PM<sub>2.5</sub>)  
328 at urban, suburban and rural background sites in the region of Paris (France). *Atmospheric*  
329 *Chemistry Physics* 13, 7825-7844.
- 330 Calvert, J.G., Lazrus, A., Kok, G.L., Heikes, B.G., Walega, J.G., Lind, J., Cantrell, C.A., 1985.  
331 Chemical mechanisms of acid generation in the troposphere. *Nature* 317, 27-35.
- 332 Cao, G.L., Zhang, X.Y., Zheng, F.C., 2006. Inventory of black carbon and organic carbon  
333 emissions from China. *Atmospheric Environment* 40, 6516-6527.
- 334 Cao, J.J., Shen, Z.X., Chow, J.C., Qi, G.W., Watson, J.G., 2009. Seasonal variations and sources  
335 of mass and chemical composition for PM<sub>10</sub> aerosol in Hangzhou, China. *Particuology* 7,  
336 161-168.
- 337 Chang, D., Song, Y., Liu, B., 2009. Visibility trends in six megacities in China 1973-2007.  
338 *Atmospheric Research* 94, 161-167.
- 339 Chen, R.J. et al., 2012a. Association of particulate air pollution with daily mortality. *American*  
340 *Journal of Epidemiology* 175, 1173-1181.
- 341 Chen, Y., Zheng, M., Edgerton, E.S., Ke, L., Sheng, G., Fu, J., 2012b. PM<sub>2.5</sub> source apportionment  
342 in the southeastern U.S.: Spatial and seasonal variations during 2001-2005. *Journal of*  
343 *Geophysical Research-Atmospheres* 117.
- 344 Choi, J.K., Heo, J.B., Ban, S.J., Yi, S.M., Zoh, K.D., 2012. Chemical characteristics of PM<sub>2.5</sub>  
345 aerosol in Incheon, Korea. *Atmospheric Environment* 60, 583-592.
- 346 Cusack, M., Alastuey, A., Perez, N., Pey, J., Querol, X., 2012. Trends of particulate matter (PM<sub>2.5</sub>)  
347 and chemical composition at a regional background site in the Western Mediterranean over  
348 the last nine years (2002-2010). *Atmospheric Chemistry and Physics* 12, 8341-8357.
- 349 Ding, Y.H., Chan, J.C.L., 2005. The East Asian summer monsoon: an overview. *Meteorology and*  
350 *Atmospheric Physics* 89, 117-142.
- 351 Du, H., Kong, L., Cheng, T., Chen, J., Du, J., Li, L., Xia, X., Leng, C., Huang, G., 2011. Insights  
352 into summertime haze pollution events over Shanghai based on online water-soluble ionic

353 composition of aerosols. *Atmospheric Environment* 45, 5131-5137.

354 Fan, S.J. et al., 2008. Meteorological conditions and structures of atmospheric boundary layer in  
355 October 2004 over Pearl River Delta area. *Atmospheric Environment* 42, 6174-6186.

356 Fu, Q. et al., 2008. Mechanism of formation of the heaviest pollution episode ever recorded in the  
357 Yangtze River Delta, China. *Atmospheric Environment* 42, 2023-2036.

358 Gu, B. et al., 2012. Atmospheric reactive nitrogen in China: sources, recent trends, and damage  
359 costs. *Environmental Science & Technology* 46, 9420-9427.

360 Guangdong Provincial Bureau of Statistics (GPBS) (2008), Guangdong Statistical Yearbook 2008,  
361 China Statistics Press, Beijing.

362 Guangdong Provincial Bureau of Statistics (GPBS) (2009), Guangdong Statistical Yearbook 2009,  
363 China Statistics Press, Beijing.

364 Guangdong Provincial Bureau of Statistics (GPBS) (2010), Guangdong Statistical Yearbook 2010,  
365 China Statistics Press, Beijing.

366 Guangdong Provincial Bureau of Statistics (GPBS) (2011), Guangdong Statistical Yearbook 2011,  
367 China Statistics Press, Beijing.

368 Guangdong Provincial Bureau of Statistics (GPBS) (2012), Guangdong Statistical Yearbook 2012,  
369 China Statistics Press, Beijing.

370 Guo, H. et al., 2009. Concurrent observations of air pollutants at two sites in the Pearl River Delta  
371 and the implication of regional transport. *Atmospheric Chemistry and Physics* 9, 7343-7360.

372 Holland, D.M., Principe, P.P., Sickles, J.E., 1999. Trends in atmospheric sulfur and nitrogen  
373 species in the eastern United States for 1989-1995. *Atmospheric Environment* 33, 37-49.

374 Hu, M., Wu, Z., Slanina, J., Lin, P., Liu, S., Zeng, L., 2008. Acidic gases, ammonia and  
375 water-soluble ions in PM<sub>2.5</sub> at a coastal site in the Pearl River Delta, China. *Atmospheric*  
376 *Environment* 42, 6310-6320.

377 Hua, W. et al., 2008. Atmospheric hydrogen peroxide and organic hydroperoxides during  
378 PRIDE-PRD'06, China: their concentration, formation mechanism and contribution to  
379 secondary aerosols. *Atmospheric Chemistry and Physics* 8, 6755-6773.

380 Jones, A.M., Harrison, R.M., 2011. Temporal trends in sulphate concentrations at European sites  
381 and relationships to sulphur dioxide. *Atmospheric Environment* 45, 873-882.

382 Jung, J., Lee, H., Kim, Y.J., Liu, X., Zhang, Y., Gu, J., Fan, S., 2009. Aerosol chemistry and the  
383 effect of aerosol water content on visibility impairment and radiative forcing in Guangzhou  
384 during the 2006 Pearl River Delta campaign. *Journal of Environmental Management* 90,  
385 3231-3244.

386 Kim, B.M., Teffera, S., Zeldin, M.D., 2000. Characterization of PM<sub>2.5</sub> and PM<sub>10</sub> in the South  
387 Coast Air Basin of southern California: Part 1 - Spatial variations. *Journal of the Air & Waste*  
388 *Management Association* 50, 2034-2044.

389 Lai, S.C., Zou, S.C., Cao, J.J., Lee, S.C., Ho, K.F., 2007. Characterizing ionic species in PM<sub>2.5</sub>  
390 and PM<sub>10</sub> in four Pearl River Delta cities, South China. *Journal of Environmental*  
391 *Sciences-China* 19, 939-947.

392 Lei, Y., Zhang, Q., He, K.B., Streets, D.G., 2011. Primary anthropogenic aerosol emission trends  
393 for China, 1990-2005. *Atmospheric Chemistry and Physics*. 11, 931-954.

394 Liu, Y., Shao, M., Lu, S., Chang, C.-C., Wang, J.-L., Fu, L., 2008. Source apportionment of  
395 ambient volatile organic compounds in the Pearl River Delta, China: Part II. *Atmospheric*

396 Environment 42, 6261-6274.

397 Lu, Q., Zheng, J.Y., Ye, S.Q., Shen, X.L., Yuan, Z.B., Yin, S.S., 2013. Emission trends and source  
398 characteristics of SO<sub>2</sub>, NO<sub>x</sub>, PM<sub>10</sub> and VOCs in the Pearl River Delta region from 2000 to  
399 2009. *Atmospheric Environment*. 76, 11-20.

400 Lu, Z., Streets, D.G., Zhang, Q., Wang, S., Carmichael, G.R., Cheng, Y.F., Wei, C., Chin, M.,  
401 Diehl, T., Tan, Q., 2010. Sulfur dioxide emissions in China and sulfur trends in East Asia  
402 since 2000. *Atmospheric Chemistry and Physics* 10, 6311-6331.

403 Lovblad, G., Tarrason, L and Torseth, K., 2004. Chapter 2: sulphur, EMEP Assessment Part 1:  
404 European Perspective. Norwegian Meteorological Institute, 25-26.

405 Manktelow, P.T., Mann, G.W., Carslaw, K.S., Spracklen, D.V., Chipperfield, M.P., 2007. Regional  
406 and global trends in sulfate aerosol since the 1980s. *Geophysical Research Letters* 34.

407 Marinoni, A., Parazols, M., Brigante, M., Deguillaume, L., Amato, P., Delort, A.M., Laj, P.,  
408 Mailhot, G., 2011. Hydrogen peroxide in natural cloud water: Sources and photoreactivity.  
409 *Atmospheric Research* 101, 256-263.

410 Merkel, A.W., Harder, J.W., Marsh, D.R., Smith, A.K., Fontenla, J.M., Woods, T.N., 2011. The  
411 impact of solar spectral irradiance variability on middle atmospheric ozone. *Geophysical*  
412 *Research Letters* 38.

413 Ohara, T., Akimoto, H., Kurokawa, J., Horii, N., Yamaji, K., Yan, X., Hayasaka, T., 2007. An  
414 Asian emission inventory of anthropogenic emission sources for the period 1980-2020.  
415 *Atmospheric Chemistry and Physics* 7, 4419-4444.

416 Qin, Y., Xie, S.D., 2012. Spatial and temporal variation of anthropogenic black carbon emissions  
417 in China for the period 1980-2009. *Atmospheric Chemistry and Physics* 12, 4825-4841.

418 Rinehart, L.R., Fujita, E.M., Chow, J.C., Magliano, K., Zielinska, B., 2006. Spatial distribution of  
419 PM<sub>2.5</sub> associated organic compounds in central California. *Atmospheric Environment* 40,  
420 290-303.

421 Shang, Y., Sun, Z.W., Cao, J.J., Wang, X.M., Zhong, L.J., Bi, X.H., Li, H., Liu, W.X., Zhu, T.,  
422 Huang, W., 2013. Systematic review of Chinese studies of short-term exposure to air  
423 pollution and daily mortality. *Environment International* 54, 100-111.

424 Seinfeld, J.H., Pandis, S.M., 2006. *Atmospheric Chemistry and Physics: From Air Pollution to*  
425 *Climate Change*, second ed. John Wiley and Sons, New York.

426 Simpson, I.J., Wang, T., Guo, H., Kwok, Y.H., Flocke, F., Atlas, E., Meinardi, S., Rowland, F.S.,  
427 Blake, D.R., 2006. Long-term atmospheric measurements of C<sub>1</sub>-C<sub>5</sub> alkyl nitrates in the pearl  
428 river delta region of southeast China. *Atmospheric Environment* 40, 1619-1632.

429 Streets, D.G., Bond, T.C., Carmichael, G.R., Fernandes, S.D., Fu, Q., He, D., Klimont, Z., Nelson,  
430 S.M., Tsai, N.Y., Wang, M.Q., Woo, J.H., Yarber, K.F., 2003. An inventory of gaseous and  
431 primary aerosol emissions in Asia in the year 2000. *Journal of Geophysical*  
432 *Research-Atmospheres* 108.

433 Sun, Y.L., Zhuang, G.S., Tang, A.H., Wang, Y., An, Z.S., 2006. Chemical characteristics of PM<sub>2.5</sub>  
434 and PM<sub>10</sub> in haze-fog episodes in Beijing. *Environmental Science & Technology* 40,  
435 3148-3155.

436 Sun, Z.Q., Mu, Y.J., Liu, Y.J., Shao, L.Y., 2013. A comparison study on airborne particles during  
437 haze days and non-haze days in Beijing. *Science of the Total Environment* 456, 1-8.

438 Tan, J.H., Duan, J.C., He, K.B., Ma, Y.L., Duan, F.K., Chen, Y., Fu, J.M., 2009a. Chemical

439 characteristics of PM<sub>2.5</sub> during a typical haze episode in Guangzhou. *Journal of*  
440 *Environmental Sciences-China* 21, 774-781.

441 Tan, J.H., Duan, J.C., Chen, D.H., Wang, X.H., Guo, S.J., Bi, X.H., Sheng, G.Y., He, K.B., Fu,  
442 J.M., 2009b. Chemical characteristics of haze during summer and winter in Guangzhou.  
443 *Atmospheric Research* 94, 238-245.

444 Tao, J., Cao, J.J., Zhang, R.J., Zhu, L., Zhang, T., Shi, S., Chan, C.Y., 2012. Reconstructed light  
445 extinction coefficients using chemical compositions of PM<sub>2.5</sub> in winter in urban Guangzhou,  
446 China. *Advances in Atmospheric Sciences* 29, 359-368.

447 Tie, X.X., Wu, D., Basseur, G., 2009. Lung cancer mortality and exposure to atmospheric aerosol  
448 particles in Guangzhou, China. *Atmospheric Environment* 43, 2375-2377.

449 Turpin, B.J., Huntzicker, J.J., 1995. Identification of secondary organic aerosol episodes and  
450 quantitation of primary and secondary organic aerosol concentrations during SCAQS.  
451 *Atmospheric Environment* 29, 3527-3544.

452 Van Donkelaar, A., Martin, R.V., Brauer, M., Kahn, R., Levy, R., Verduzco, C., Villeneuve, P.J.,  
453 2010. Global estimates of ambient fine particulate matter concentrations from satellite-based  
454 aerosol optical depth: development and application. *Environmental Health Perspectives* 118,  
455 847-855.

456 Wang, B., Shao, M., Roberts, J.M., Yang, G., Yang, F., Hu, M., Zeng, L.M., Zhang, Y.H., Zhang,  
457 J.B., 2010. Ground-based on-line measurements of peroxyacetyl nitrate (PAN) and  
458 peroxypropionyl nitrate (PPN) in the Pearl River Delta, China. *International Journal of*  
459 *Environmental Analytical Chemistry* 90, 548-559.

460 Wang, X. et al., 2012a. Aerosol scattering coefficients and major chemical compositions of fine  
461 particles observed at a rural site hit the central Pearl River Delta, South China. *Journal of*  
462 *Environmental Sciences-China* 24, 72-77.

463 Wang, X. et al., 2012b. Characteristics of surface ozone at an urban site of Xi'an in Northwest  
464 China. *Journal of Environmental Monitoring* 14, 116-126.

465 Wang, Y., Zhuang, G., Xu, C., An, Z., 2007. The air pollution caused by the burning of fireworks  
466 during the lantern festival in Beijing. *Atmospheric Environment* 41, 417-431.

467 Wang, Y., Zhuang, G.S., Tang, A.H., Yuan, H., Sun, Y.L., Chen, S.A., Zheng, A.H., 2005. The ion  
468 chemistry and the source of PM<sub>2.5</sub> aerosol in Beijing. *Atmospheric Environment* 39,  
469 3771-3784.

470 Wu, D. et al., 2005. An extremely low visibility event over the Guangzhou region: A case study.  
471 *Atmospheric Environment* 39, 6568-6577.

472 Yang, F., Tan, J., Zhao, Q., Du, Z., He, K., Ma, Y., Duan, F., Chen, G., 2011. Characteristics of  
473 PM<sub>2.5</sub> speciation in representative megacities and across China. *Atmospheric Chemistry and*  
474 *Physics* 11, 5207-5219.

475 Yao, X.H., Chan, C.K., Fang, M., Cadle, S., Chan, T., Mulawa, P., He, K.B., Ye, B.M., 2002. The  
476 water-soluble ionic composition of PM<sub>2.5</sub> in Shanghai and Beijing, China. *Atmospheric*  
477 *Environment* 36, 4223-4234.

478 Zhang, Q., He, K.B., Huo, H., 2012a. Cleaning China's air. *Nature* 484, 161-162.

479 Zhang, X., van Geffen, J., Liao, H., Zhang, P., Lou, S., 2012b. Spatiotemporal variations of  
480 tropospheric SO<sub>2</sub> over China by SCIAMACHY observations during 2004-2009. *Atmospheric*  
481 *Environment* 60, 238-246.

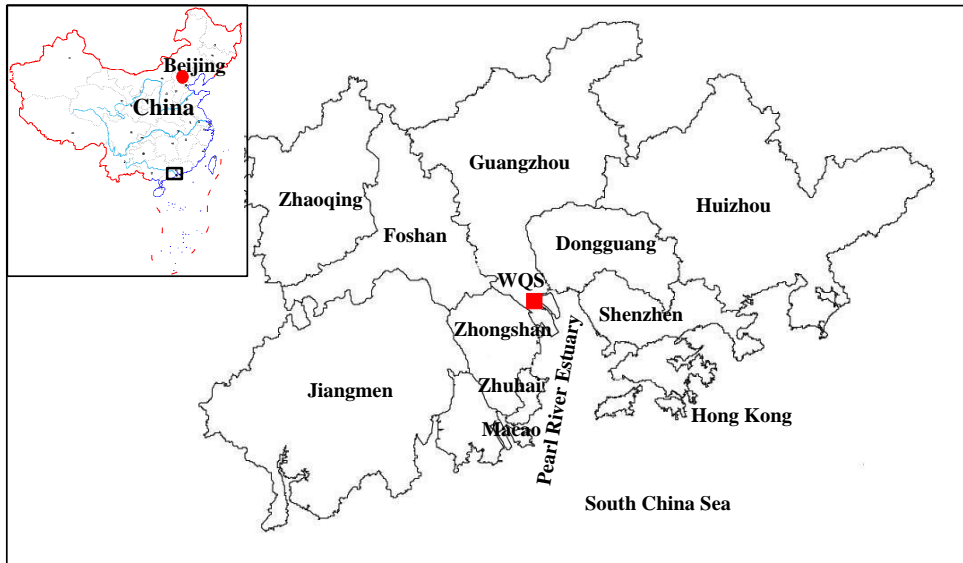


- 482 Zhao, Y., Wang, S., Duan, L., Lei, Y., Cao, P., Hao, J., 2008. Primary air pollutant emissions of  
483 coal-fired power plants in China: Current status and future prediction. *Atmospheric*  
484 *Environment* 42, 8442-8452.
- 485 Zheng, J., Zhang, L., Che, W., Zheng, Z., Yin, S., 2009. A highly resolved temporal and spatial air  
486 pollutant emission inventory for the Pearl River Delta region, China and its uncertainty  
487 assessment. *Atmospheric Environment* 43, 5112-5122.
- 488 Zheng, J., He, M., Shen, X., Yin, S., Yuan, Z., 2012. High resolution of black carbon and organic  
489 carbon emissions in the Pearl River Delta region, China. *The Science of the total*  
490 *environment* 438, 189-200.
- 491

492 Table 1. Concentration of PM<sub>2.5</sub> mass, carbonaceous and ionic species in fall and winter from  
 493 2007 to 2011 (average  $\pm$  95% confidence interval) (unit:  $\mu\text{g}/\text{m}^3$ )

Year/Species	10/23-	11/10-	11/25-	11/01-	11/11-
	11/24/2007	12/09/2008	12/23/2009	12/26/2010	12/11/2011
PM <sub>2.5</sub>	112.5 $\pm$ 8.2	103.8 $\pm$ 9.9	95.0 $\pm$ 9.5	88.9 $\pm$ 9.2	78.6 $\pm$ 7.6
OC	19.3 $\pm$ 1.7	22.7 $\pm$ 2.9	17.2 $\pm$ 2.8	18.3 $\pm$ 2.1	15.2 $\pm$ 2.1
EC	3.6 $\pm$ 0.4	4.2 $\pm$ 0.4	5.5 $\pm$ 0.9	3.3 $\pm$ 0.4	3.1 $\pm$ 0.4
SO <sub>4</sub> <sup>2-</sup>	22.7 $\pm$ 2.3	15.7 $\pm$ 2.0	17.0 $\pm$ 2.4	17.2 $\pm$ 2.0	14.2 $\pm$ 1.8
NO <sub>3</sub> <sup>-</sup>	6.7 $\pm$ 1.1	8.8 $\pm$ 1.8	11.5 $\pm$ 1.9	10.9 $\pm$ 2.1	9.6 $\pm$ 1.5
Na <sup>+</sup>	0.8 $\pm$ 0.1	1.0 $\pm$ 0.2	0.9 $\pm$ 0.1	0.6 $\pm$ 0.1	0.6 $\pm$ 0.1
NH <sub>4</sub> <sup>+</sup>	6.5 $\pm$ 0.6	5.4 $\pm$ 0.9	7.1 $\pm$ 0.9	7.5 $\pm$ 1.1	6.6 $\pm$ 0.9
K <sup>+</sup>	1.5 $\pm$ 0.2	1.7 $\pm$ 0.3	1.0 $\pm$ 0.2	1.4 $\pm$ 0.2	1.1 $\pm$ 0.2
Mg <sup>2+</sup>	0.2 $\pm$ 0.02	0.1 $\pm$ 0.01	0.2 $\pm$ 0.04	0.1 $\pm$ 0.04	0.1 $\pm$ 0.01
Ca <sup>2+</sup>	1.3 $\pm$ 0.2	1.1 $\pm$ 0.2	0.3 $\pm$ 0.1	0.4 $\pm$ 0.1	0.5 $\pm$ 0.1
Cl <sup>-</sup>	1.0 $\pm$ 0.2	1.5 $\pm$ 0.5	1.8 $\pm$ 0.4	1.9 $\pm$ 0.5	1.5 $\pm$ 0.4
OC/EC	5.8 $\pm$ 0.6	5.4 $\pm$ 0.5	3.2 $\pm$ 0.2	5.6 $\pm$ 0.3	4.9 $\pm$ 0.3
[NH <sub>4</sub> <sup>+</sup> ]/[SO <sub>4</sub> <sup>2-</sup> ] <sup>a</sup>	1.6 $\pm$ 0.2	1.8 $\pm$ 0.2	2.3 $\pm$ 0.2	2.4 $\pm$ 0.2	2.5 $\pm$ 0.2
[NH <sub>4</sub> <sup>+</sup> ]/2×[SO <sub>4</sub> <sup>2-</sup> ]+[NO <sub>3</sub> <sup>-</sup> ] <sup>a</sup>	0.64 $\pm$ 0.04	0.63 $\pm$ 0.05	0.73 $\pm$ 0.02	0.78 $\pm$ 0.05	0.80 $\pm$ 0.02
[NO <sub>3</sub> <sup>-</sup> ]/[SO <sub>4</sub> <sup>2-</sup> ]	0.31 $\pm$ 0.1	0.58 $\pm$ 0.1	0.73 $\pm$ 0.1	0.65 $\pm$ 0.1	0.70 $\pm$ 0.1
RH (%)	68.1 $\pm$ 3.4	43.6 $\pm$ 4.3	67.2 $\pm$ 5.3	70.5 $\pm$ 2.8	70.7 $\pm$ 3.7
T (°C)	22.5 $\pm$ 0.8	17.7 $\pm$ 1.1	17.1 $\pm$ 1.3	19.9 $\pm$ 1.0	20.2 $\pm$ 1.5
WS (m/s)	1.2 $\pm$ 0.1	1.3 $\pm$ 0.1	1.7 $\pm$ 0.1	2.3 $\pm$ 0.1	1.8 $\pm$ 0.1

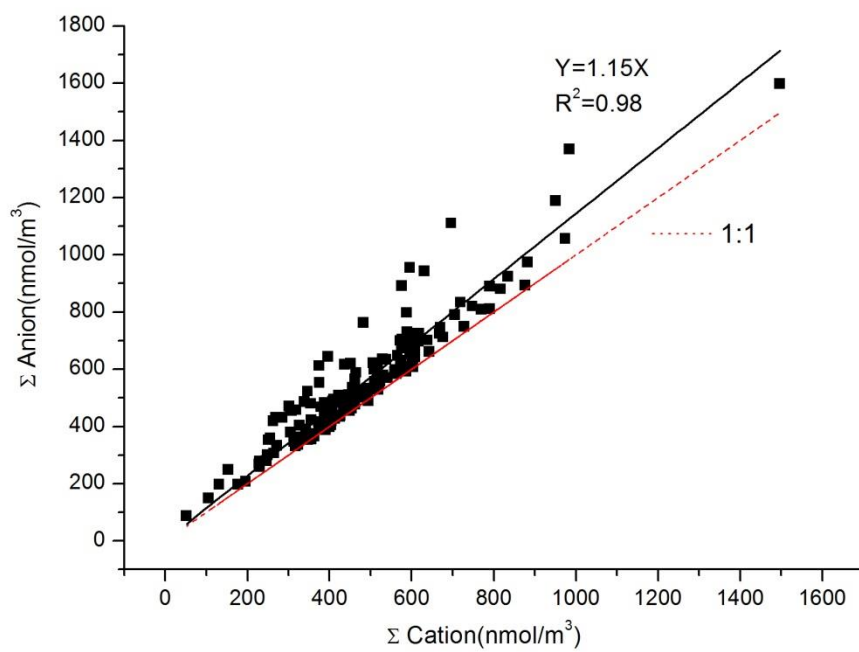
494 <sup>a</sup> Ratio of nmol m<sup>-3</sup>



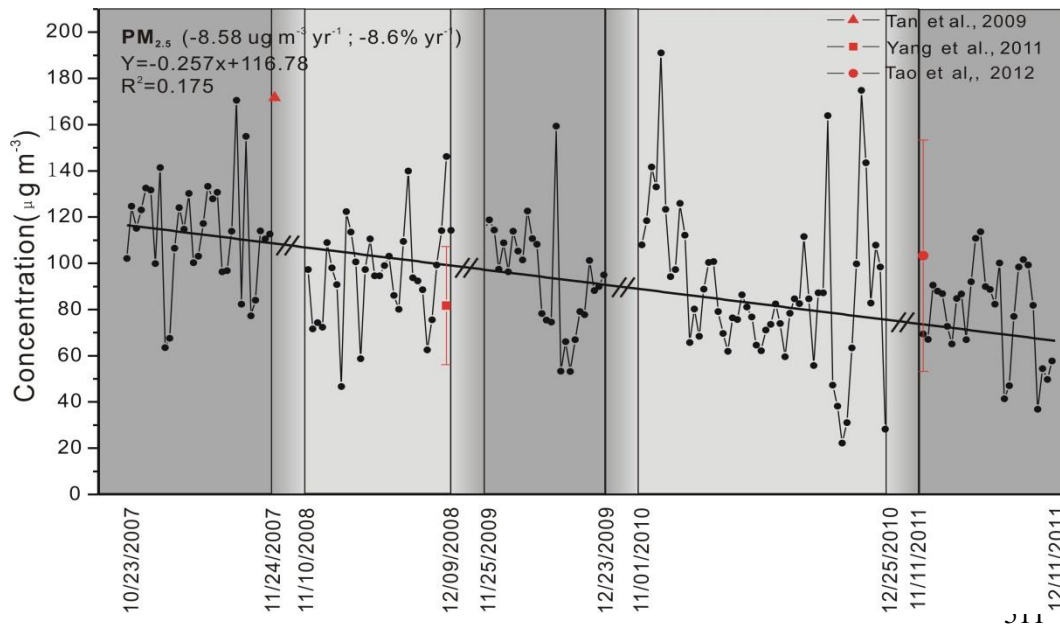
495

496

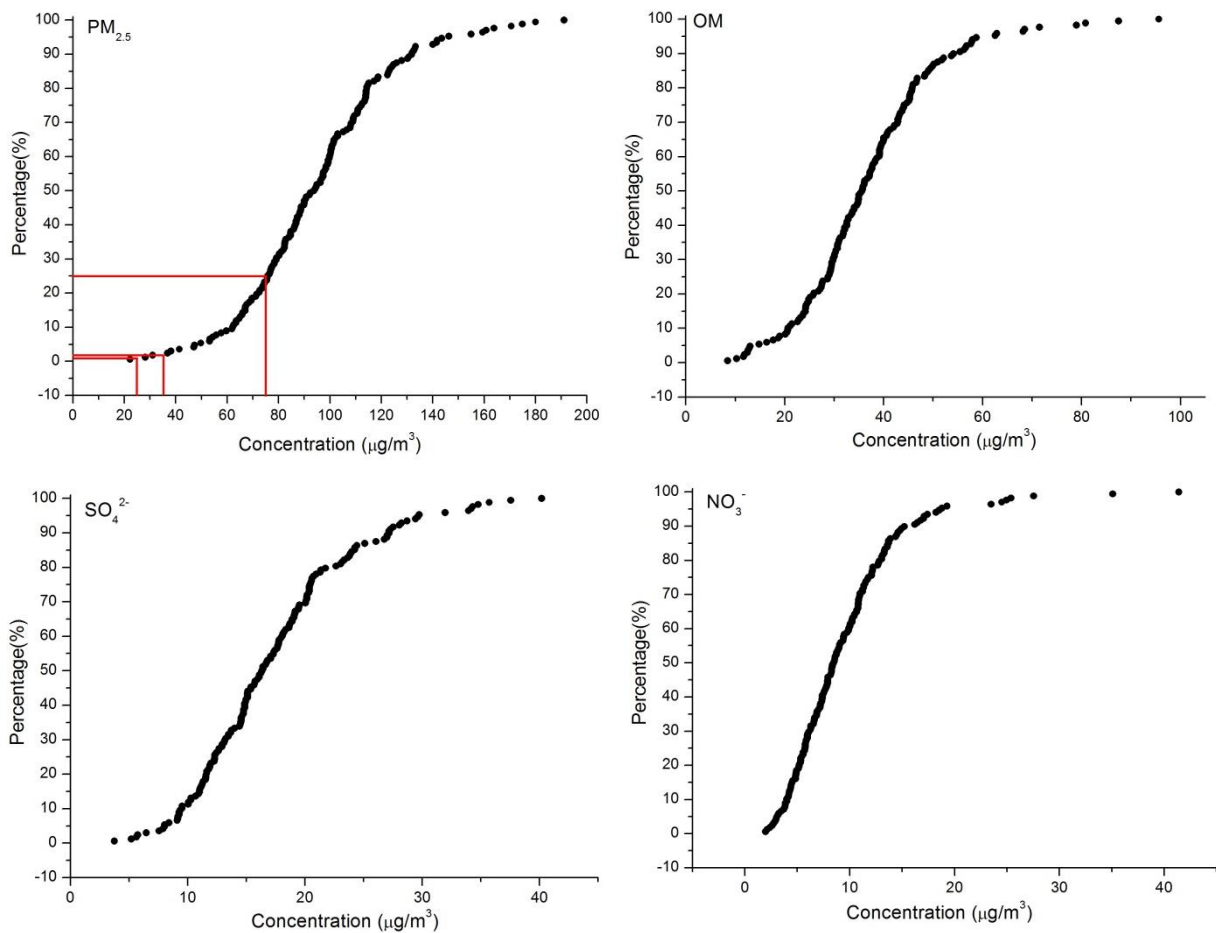
497 Figure 1. Location of the sampling site Wanqingsha (WQS) and its surrounding environments



498  
499 Figure 2. Charge balance between cations and anions in all PM<sub>2.5</sub> samples  
500  
501



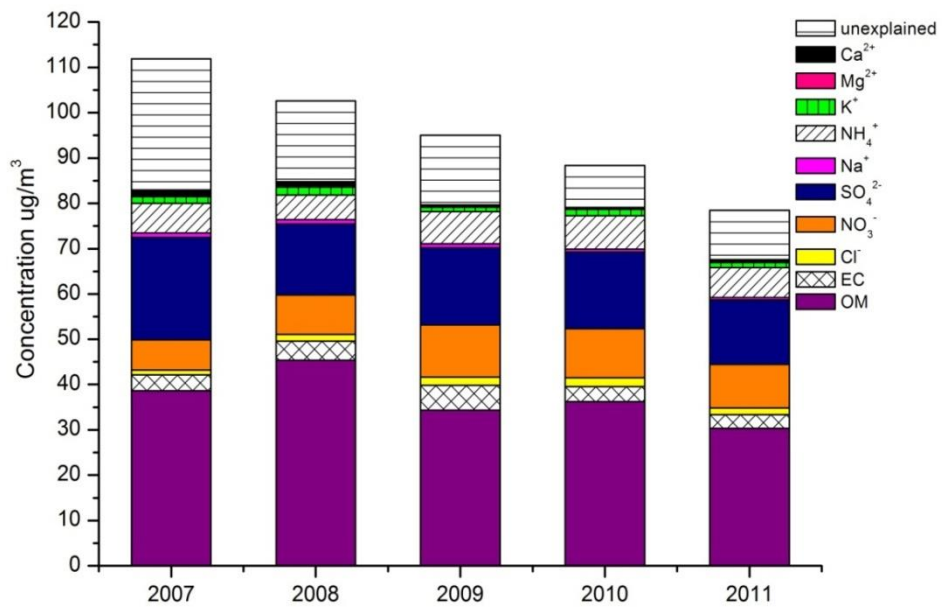
512 Figure 3. Annual variation of  $PM_{2.5}$  mass concentration in fall and winter from 2007 to 2011



513

514 Figure 4. The cumulative percentage of PM<sub>2.5</sub>, OM, SO<sub>4</sub><sup>2-</sup> and NO<sub>3</sub><sup>-</sup> mass concentrations in fall  
 515 and winter from 2007 to 2011. The red lines are the different PM<sub>2.5</sub> mass concentration standards:  
 516 WHO 24-hr guideline (25 µg m<sup>-3</sup>), USEPA 24-hr standard (35 µg m<sup>-3</sup>) and China's new national  
 517 ambient air quality daily standard guideline (75 µg m<sup>-3</sup>).

518



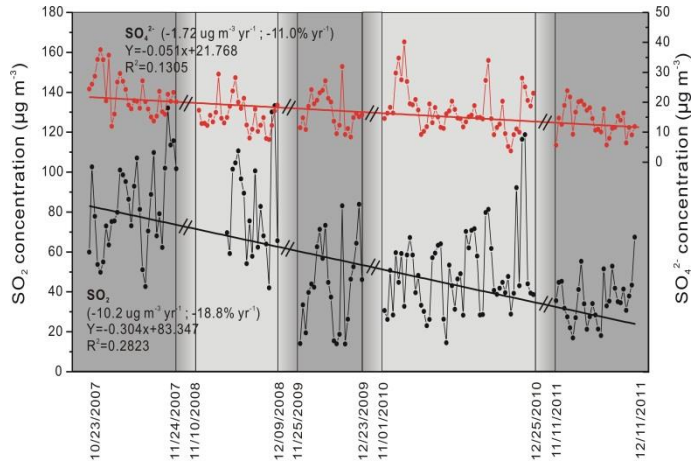
519

520 Figure 5. PM<sub>2.5</sub> components in fall and winter from 2007 to 2011

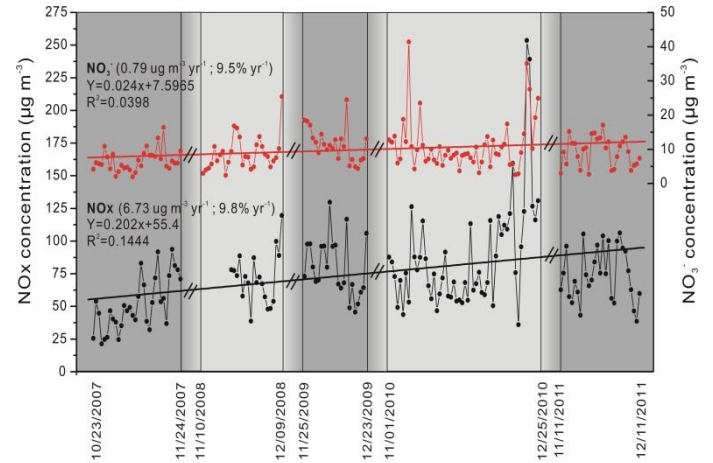
521

522

(a)



(b)



523

524 Figure 6. Annual variation of (a) sulfate ( $\text{SO}_4^{2-}$ ) (red dots) and sulfur dioxide ( $\text{SO}_2$ ) (black dot),  
 525 and (b) nitrate ( $\text{NO}_3^-$ ) (red dot) and nitrogen oxide ( $\text{NO}_x$ ) (black dot) in fall and winter from 2007  
 526 to 2011.

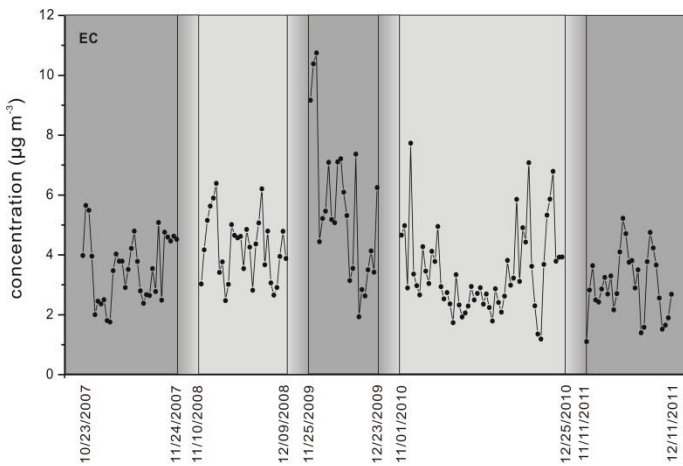
527

528

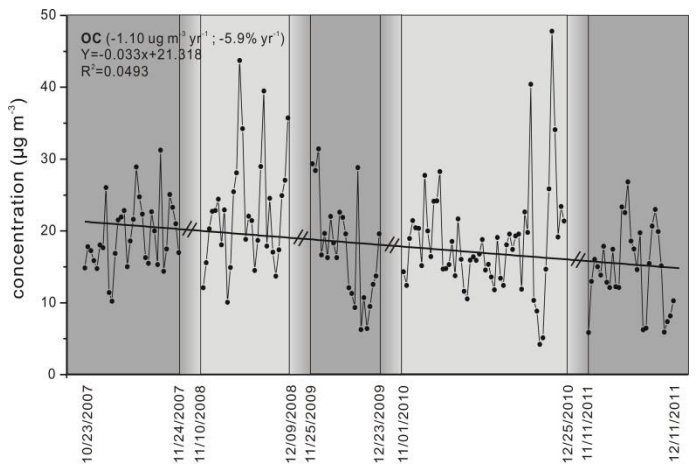
529

530

(a)



(b)



531

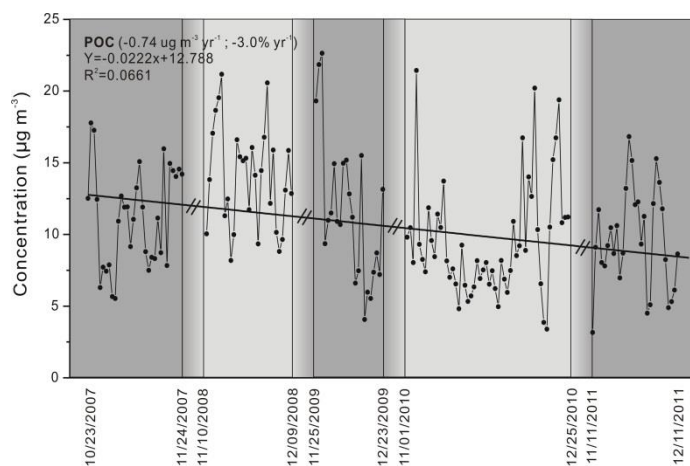
532 Figure 7. Annual variation of (a) elemental carbon (EC) and (b) organic carbon (OC) in fall and  
 533 winter from 2007 to 2011

534

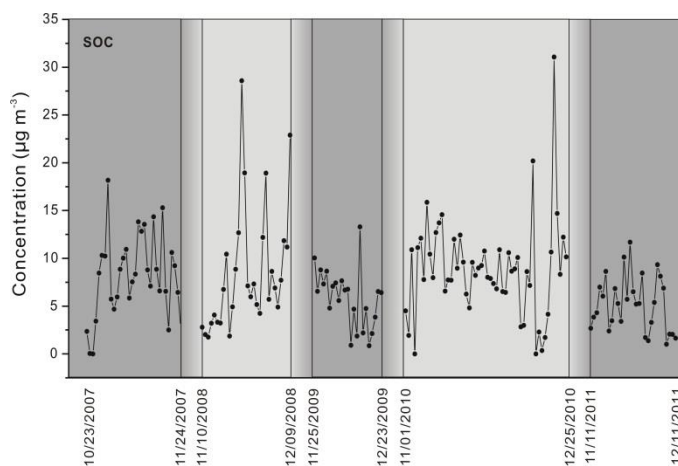
535



536 (a)



(b)



537

538 Figure 8. Annual variation of (a) primary organic carbon (POC) and (b) secondary organic carbon

539 (SOC) in fall and winter from 2007 to 2011

540

541

542